


# Chlamydial virulence factor TarP mimics talin to disrupt the talin-vinculin complex

Austin J. Whitewood, Abhimanyu K. Singh, David G. Brown and Benjamin T. Goult 

School of Biosciences, University of Kent, Canterbury, UK

## Correspondence

B. T. Goult, School of Biosciences,  
University of Kent, Canterbury, Kent, CT2  
7NJ, UK  
E-mail: b.t.goult@kent.ac.uk

(Received 8 March 2018, revised 12 April  
2018, accepted 21 April 2018, available  
online 15 May 2018)

doi:10.1002/1873-3468.13074

Edited by Stuart Ferguson

**Vinculin is a central component of mechanosensitive adhesive complexes that form between cells and the extracellular matrix. A myriad of infectious agents mimic vinculin binding sites (VBS), enabling them to hijack the adhesion machinery and facilitate cellular entry. Here, we report the structural and biochemical characterisation of VBS from the chlamydial virulence factor TarP. Whilst the affinities of isolated VBS peptides from TarP and talin for vinculin are similar, their behaviour in larger fragments is markedly different. In talin, VBS are cryptic and require mechanical activation to bind vinculin, whereas the TarP VBS are located in disordered regions, and so are constitutively active. We demonstrate that the TarP VBS can uncouple talin:vinculin complexes, which may lead to adhesion destabilisation.**

**Keywords:** adhesion; chlamydia; crystallography; molecular mimicry; talin; vinculin

Interactions between cells and the surrounding extracellular matrix (ECM), mediated *via* the integrin family of cell adhesion molecules, are fundamental to the development of multicellular life. These adhesions serve not just as attachment points but also as mechanosensitive signalling hubs, enabling cells to sense and respond to the external environment. Integrin receptors bound to ECM are coupled to the actin cytoskeleton *via* the mechanosensitive protein talin [1]. Under force, helical bundles in the talin rod domain unfold, exposing multiple cryptic vinculin binding sites (VBS) [2,3] that bind to the vinculin head (Vd1), activating autoinhibited vinculin by displacing the vinculin tail [4] (Fig. 1A). Activation of talin and vinculin also exposes numerous other cryptic binding sites for ligands that affect the assembly and regulation of both cell:ECM focal adhesions (FAs) and cell:cell junctions [5,6].

These highly conserved attachment points linking the cell to the outside world have also become

recognition sites for numerous infectious agents [7,8] with some bacteria specifically targeting adhesion proteins for cellular entry. It has previously been shown that the *Shigella flexneri* effector protein IpaA [9] and the *Rickettsia* cell surface antigen Sca4 interact with vinculin [10]. The atomic structures of these virulence factors reveal mimicry of the talin VBS. Thus, by forming amphipathic  $\alpha$ -helices that bind to Vd1, these virulence factors activate autoinhibited vinculin and hijack cell adhesion to aid pathogenesis.

Chlamydia invasion has been shown to require the effector protein translocated actin recruiting protein (TarP) which is thought to play an important role in actin recruitment [11,12]. TarP is translocated into the host cell by a chlamydial type 3 secretory system upon early elementary body (EB) attachment to the host cell. TarP injection by the bacteria leads to the recruitment and bundling of actin filaments at the point of invasion [12]. Recently, Thwaites *et al.* reported the presence of a vinculin binding region in TarP,

## Abbreviations

FP, fluorescence polarisation; HSQC, heteronuclear single quantum coherence; LD-motif, leucine-aspartic acid motif; TarP, translocated actin recruitment protein; VBS, vinculin-binding site.

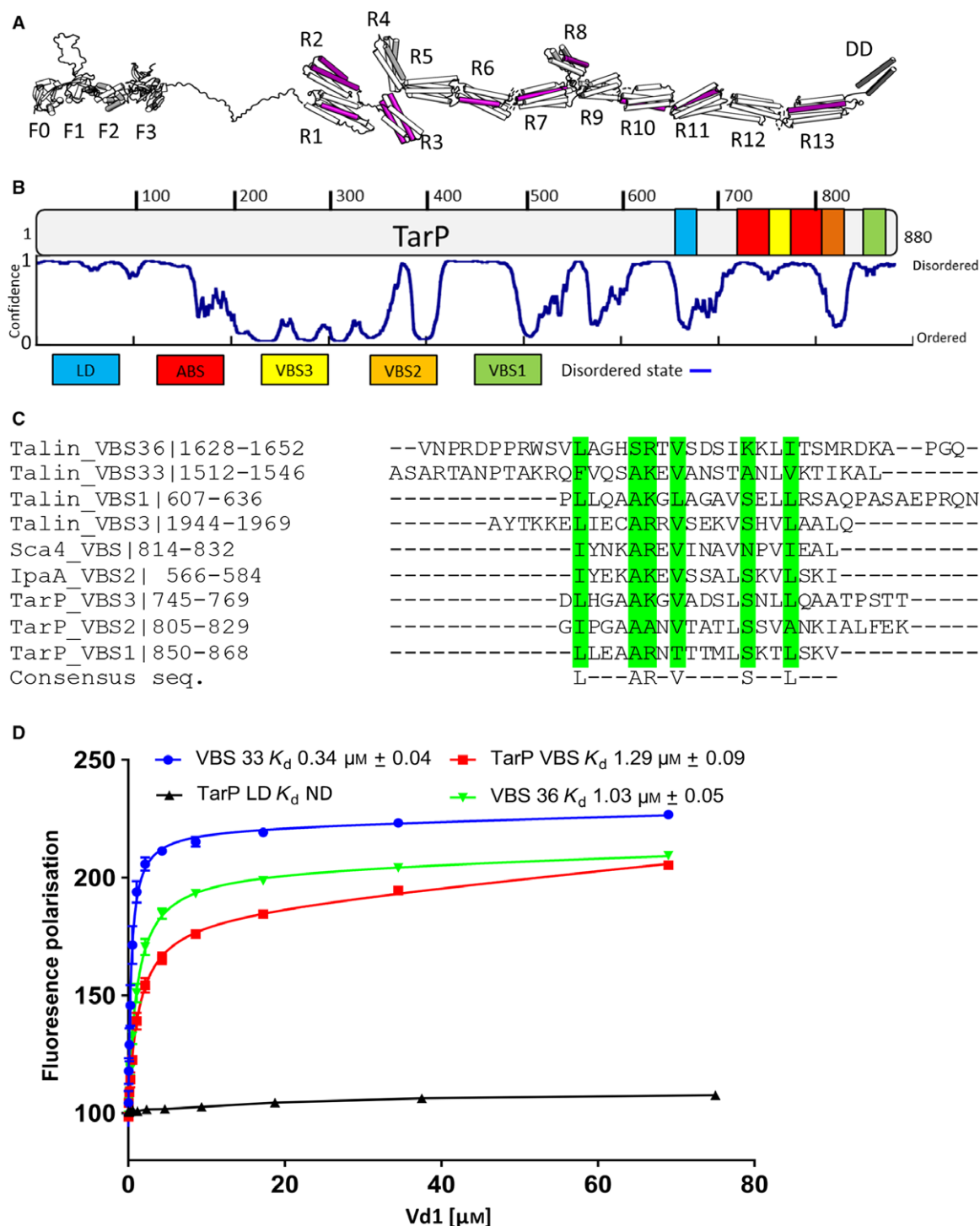


**Fig. 1.** Biochemical characterisation of the TarP interaction with the vinculin head (Vd1). (A) Schematic of talin structure, with the location of the 11 talin VBS indicated (purple). (B) Schematic of TarP, indicating locations of VBS1 (green), VBS2 (orange), VBS3 (yellow), Actin binding site ABS (red) and LD-motif (blue) at the C-terminal. The disorder prediction trace generated using DISOPRED3 [44] is shown. (C) Multiple sequence alignment of vinculin binding sites, aligned using Clustal Omega. The consensus residues are highlighted in green. (D) Comparison of the Vd1:TarP and Vd1:talin interactions. Binding of fluorescein labelled talin VBS33, VBS36, TarP VBS (850–868)C and LD (655–680)C peptides to Vd1, measured using a fluorescence polarisation assay. Dissociation constants  $\pm$  SE ( $\mu\text{M}$ ) for the interactions are indicated in the legend. All measurements were performed in triplicate. ND, not determined.

containing three vinculin binding sites (VBS) with 'VBS1' being essential for vinculin recruitment [13]. Additionally, TarP was reported to contain a Leucine-Aspartic acid motif (LD-motif) with a similar consensus sequence to the second paxillin LD-motif (LD2) which interacts with focal adhesion kinase (FAK) [14], and thus may provide TarP with a means of engaging FAK and altering cell adhesion signalling.

Here, we report the structure of the TarP:vinculin Vd1 complex and biochemically characterise and compare the interaction of the TarP VBS and talin VBS with vinculin. Whilst the affinities of the isolated VBS from TarP and talin are similar, their behaviour in larger polypeptide fragments is very different. Thus, the TarP VBS are positioned in unstructured regions, and TarP VBS1 is constitutively active whilst the talin VBS are buried inside folded rod domains and are cryptic. Furthermore, we demonstrate TarP VBS1 disrupts talin:vinculin complexes *in vitro*. This ability to uncouple vinculin from talin suggests that TarP and other virulence factors may have the capacity to trigger FA disassembly during invasion.

## Materials and methods

### Expression of recombinant polypeptides

Chicken vinculin Vd1 (residues 1–259), murine talin R10 (residues 1815–1973), and the FAK-FAT domain (residues 941–1090) were cloned into a pET151 vector (Invitrogen) and expressed in *E. coli* BL21 (DE3) cells cultured in LB. Standard nickel-affinity chromatography was used to purify the His-tagged recombinant proteins as described previously [15]. The proteins were further purified using anion-exchange chromatography following cleavage of the 6xHis-tag with TEV protease. Protein concentrations were determined using the respective extinction coefficients at 280 nm.

### Fluorescence polarisation assays

Peptides with either a C- or N-terminal cysteine were synthesised by GLBiochem (China).

TarP\_VBS1 (LLEAARNTTTMLSKTLSKV-C; *C. caviae* residues 850–868)

TarP\_LD (EGAEGLEHLLPQLRSHLDDAFDQQGN-C; *C. caviae* residues 655–680)

Pax\_LD2 (C-NLSELDRLLELN; paxillin residues 141–153)

Pax\_LD4 (C-ATREDELMASLS; paxillin residues 262–274)

mTali\_VBS33 (C-ASARTANPTAKRQFVQSAKE-VANSTANLVKTIKAL; talin residues 1512–1546)

mTali\_VBS36 (C-VNPRDPPRWSVLGHSRTVSD-SIKKLITSMRDKAP; talin residues 1622–1656)

Peptides were coupled to a thiol-reactive fluorescein dye *via* the terminal cysteine. Stock solutions were made in phosphate-buffered saline (PBS; 137 mM NaCl, 27 mM KCl, 100 mM Na<sub>2</sub>HPO<sub>4</sub>, 18 mM KH<sub>2</sub>PO<sub>4</sub>, pH 7.4), 1 mM TCEP and 0.05% Triton X-100. Excess dye was removed using a PD-10 desalting column (GE Healthcare, Chicago, IL, USA). Titrations were performed in PBS using a constant 1 μM concentration of fluorescein-coupled peptide with increasing concentration of protein; final volume 100 μL in a black 96-well plate. Fluorescent polarisation (FP) measurements were recorded on a BMGLabTech CLARIOstar plate reader at room temperature and analysed using GraphPad Prism. *K<sub>d</sub>* values were calculated with nonlinear curve fitting using a one-site total binding model.

### Analytical gel filtration

Gel filtration was performed using a Superdex-75 size-exclusion chromatography column (GE healthcare) at a flow rate of 1 mL·min<sup>-1</sup> at 4 °C in 50 mM Tris pH 7.5, 150 mM NaCl, 2 mM DTT. A sample of 100 μL was run consisting of 100 μM of each protein/peptide, incubated at a 1 : 1 (talin:Vd1) or 1 : 1 : 1 (talin:Vd1:TarP VBS1/talin VBS36) ratio, at 37 °C for 30 min. In the competition experiment, an additional 30 nM of fluorescein-coupled TarP peptide was added to visualise the TarP elution *via* absorbance at 494 nm. The elution absorbance was measured at three wavelengths: 220 nm, 280 nm and 494 nm (fluorescein absorbance). Elution was monitored by a Malvern Viscotek SEC-MALS-9 (Malvern Panalytical, Malvern, UK). Molar mass, refractive index and weight fraction (%) were determined using the OmniSEC software (Malvern Panalytical) and statistical significance assessed using a *T*-test.

### X-ray crystallography

Crystallisation trials for Vd1 in the presence of TarP VBS peptide were conducted at 21 °C by hanging drop vapour diffusion while maintaining a 1 : 1 protein to peptide ratio. Crystals were obtained in a condition containing 0.1 M sodium citrate tribasic dehydrate pH 5.6 and 20% v/v 2-propanol. Crystals were cryoprotected in the same solution supplemented with 20% v/v glycerol prior to vitrification in liquid nitrogen. Diffraction dataset was collected at 100 K on beamline I03 at Diamond Light Source (Didcot, UK) using a Pilatus3 6M detector (Dectris, Baden, Switzerland). Crystallographic data were processed by autoPROC [16], which incorporates XDS [17], AIMLESS [18] and TRUNCATE [19] for data integration, scaling and merging. Structure of the Vd1/TarP complex was determined using chicken vinculin head as template (PDB: 3ZDL [20]) for

molecular replacement search carried out with PHASER [21]. Manual model adjustment and refinement were performed with COOT [22] and REFMAC [23] respectively. Model was validated with MOLPROBITY [24] and interaction properties were determined by PISA [25]. Figure preparation was carried out with PYMOL (Schrödinger LLC, Cambridge MA, USA). For data collection, phasing and refinement statistics, Table 1. The structure has been deposited to RCSB Protein Data Bank with accession code 6FQ4.

## NMR Spectroscopy

NMR spectra were obtained using a Bruker AVANCE III 600 MHz spectrometer equipped with CryoProbe. Experiments were performed at 298 K in 20 mM sodium phosphate pH 6.5, 50 mM NaCl, 2 mM DTT with 5% (v/v)

**Table 1.** X-ray data collection and refinement statistics for TarP-Vd1 complex. Data collected from a single crystal.

Data collection	
Synchrotron and Beamline	Diamond Light Source; I03
Space group	$P2_12_12$
Molecule/a.s.u	1
Cell dimensions	
<i>a</i> , <i>b</i> , <i>c</i> (Å)	51.80, 66.87, 95.83
$\alpha$ , $\beta$ , $\gamma$ (°)	90, 90, 90
Resolution (Å)	95.83–2.9 (2.96–2.9) <sup>a</sup>
<i>R</i> <sub>merge</sub>	0.156 (0.806)
<i>I</i> / $\sigma$ <i>I</i>	8.1 (2.5)
<i>CC</i> (1/2)	0.994 (0.903)
Completeness (%)	99.8 (99.9)
Redundancy	6.1 (6.3)
Refinement	
Resolution (Å)	2.9
No. reflections	7455 (519)
<i>R</i> <sub>work</sub> / <i>R</i> <sub>free</sub>	0.28/0.34
No. atoms	
Protein	2082
Water	3
<i>B</i> -factors (Å <sup>2</sup> )	
Protein/Peptide	94.24/95.73
Water	84.04
R.m.s. deviations	
Bond lengths (Å)	0.010
Bond angles (°)	1.430
Ramachandran plot	
Favoured/allowed/outlier (%)	93/6/1
Rotamer	
Favoured/poor (%)	59.2/21.01
Molprobit scores	
Protein geometry	3.42 (37th) <sup>b</sup>
Clash score all atoms	29 (81st) <sup>b</sup>
PDB accession no.	6FQ4

<sup>a</sup>Values in parentheses are for highest-resolution shell.

<sup>b</sup>Values in parentheses indicate percentile scores as determined by Molprobit.

<sup>2</sup>H<sub>2</sub>O. Ligand binding was evaluated from <sup>1</sup>H,<sup>15</sup>N-HSQC chemical shift changes using 130 μM <sup>15</sup>N-labelled FAK-FAT domain. Peptides were added at a 3 : 1 peptide:protein ratio.

## Results

### Chlamydial VBS interacts with vinculin

It has previously been shown that the interaction between TarP and vinculin is required for Chlamydia infection [13]. TarP was shown to contain three VBS with only the C-terminal VBS, VBS1, being critical for TarP function (Fig. 1B). Multiple sequence alignment with the VBS of talin (Fig. 1C) confirmed the region that contains the vinculin head domain (Vd1) consensus binding motif LxxAAxxVxVxxLxxA [26] as reported previously [13].

To evaluate how the interaction of Vd1 with the TarP VBS1 compares to its interaction with talin VBS, we measured the relative binding affinities using an *in vitro* fluorescence polarisation (FP) assay. In this assay, synthetic VBS peptides (Materials and methods) were fluorescently labelled with fluorescein and titrated against an increasing concentration of Vd1. Binding of the VBS peptide to Vd1 results in an increase in fluorescence polarisation (Fig. 1D), which can be used to determine the binding constant, *K*<sub>d</sub>. The TarP VBS1 peptide bound to Vd1 with an affinity of 1.29 μM. The talin VBS located on talin helices, 33 and 36 (VBS33 and VBS36), bound with comparable affinities of 0.34 μM and 1.03 μM respectively (Fig. 1D). The TarP LD region (residues 655–680), which does not interact with Vd1, was used as a negative control.

Although the affinity of the TarP VBS1 for vinculin is comparable to the VBS in talin, the location of the VBS are markedly different between the two proteins. Talin VBS are maintained in a cryptic conformation, buried inside the hydrophobic core of the talin rod domain bundles [27], and require exposure by mechanical force across talin to unfold the bundles [3,28]. In contrast, the VBS in TarP are situated in disordered regions of the molecule and are therefore likely to be constitutively active (Fig. 1B). The affinity of talin VBS in folded rod domains for Vd1 is significantly lower due to the energy required to unfold the domain to expose the VBS [29]. However, this reduced affinity of talin for vinculin is rapidly overcome by force exerted on talin, an effect that is readily reversible when force is removed, meaning that the talin:vinculin interactions are exquisitely force-dependent [28]. Therefore, in the absence of mechanical force, TarP has the potential to outcompete folded talin to bind vinculin.



### The structure of TarP VBS1 in complex with the vinculin head

To further characterise the interaction between TarP VBS1 and vinculin, we crystallised a complex of TarP (850–868) with vinculin Vd1. The crystals containing one molecule of the complex in the asymmetric unit were in orthorhombic space group  $P2_12_12$  and diffracted to a useful resolution of 2.9 Å.

The structure of the complex was determined by molecular replacement (Fig. 2A; statistics in Table 1) and shows good agreement with the complexes of Vd1 with other VBS from talin [4,30], sca-4 [31] and IpaA [32]. The TarP VBS1 forms an  $\alpha$ -helix that embeds into the hydrophobic groove formed between  $\alpha$ -helices 1 and 2 of the Vd1 N-terminal 4-helix bundle, forming a structure that resembles a five-helix bundle (Fig. 2B). Analysis of the complex interface by PISA indicated that 54.1% of the VBS surface area, including the consensus residues, is buried in the complex interface (Fig. 2A). Furthermore, two hydrogen bonds were identified: TarP Arg-855 to Vd1 Ser-11, and TarP Ser-862 to Vd1 Gln-18. Structural alignment of known VBS structures indicates that these hydrogen bonds are well conserved. Upon complex formation, TarP significantly alters the positions of Vd1 helices 1 and 2, widening the groove between the two and exposing the hydrophobic core (Fig. 2C), mimicking the way talin activates vinculin, causing the release of the vinculin tail [4,33]. With sidechains almost identical in length and character to talin VBS, TarP VBS1 is able to pack tightly into the Vd1 hydrophobic groove accounting for the high affinity we measured (Fig. 1C). The strong resemblance of the TarP VBS1 to the VBS in talin demonstrates the molecular mimicry employed by TarP to hijack the host cell adhesion machinery.

### The TarP peptide competes with talin for binding to vinculin

Since TarP VBS1 binds to the same site on vinculin as the talin VBS, this raises the possibility that TarP binding might compete with talin for vinculin binding. A similar phenomenon was seen in *Drosophila* recently, where expression of a GFP-VBS construct was found to disrupt talin:vinculin interactions *in vivo* [34]. Using analytical gel filtration, we measured the interaction between Vd1 and a VBS-containing talin helical bundle. We selected talin rod domain R10, which contains a single VBS (VBS46) [35]. Equimolar amounts of Vd1 and talin R10 incubated together at 37 °C formed a 1 : 1 complex (Fig. 3A-B). Adding a stoichiometric amount of TarP VBS1 peptide

(Fig. 3A), or a peptide of an isolated talin VBS (VBS36; Fig. 3B) resulted in a significant reduction in the talin:Vd1 peak and concomitant increases in the monomer peaks of the respective proteins. To confirm that disruption of the talin:Vd1 complex was due to competition by the TarP VBS1 peptide, we spiked the TarP VBS1 peptide with 30 nM of fluorescein-TarP VBS1 peptide (as used in the FP assay). The fluorescein-coupled TarP VBS1 eluted in the same fractions as Vd1, confirming that the TarP peptide was bound to Vd1. To quantitate this competition, we used the SEC-MALS OmniSEC software to determine the weight fraction (%) of each peak in Fig. 3A-B and this analysis is shown in Fig. 3C. This demonstrates that TarP, and exposed VBS in general, can out-compete talin for binding to Vd1 *in vitro* even when the vinculin:talin complex is already formed. Whilst the isolated talin VBS and TarP VBS1 peptides have similar affinities, the affinity of Vd1 for the intact talin rod domain is reduced significantly due to the cryptic nature of talin VBS in the folded talin helical bundles [29]. As a consequence, the constitutively active nature of the TarP VBS allows it to disrupt vinculin:talin complexes. Vinculin binding to talin inhibits talin refolding [28] and is important for FA stabilisation. TarP disruption of this complex could lead to the loosening of adhesion by disrupting the talin:vinculin:actin cytoskeletal connection. This may mean that, as well as providing a means of entry and a mechanism to hijack the actin machinery, infection might also destabilise FAs at the point of entry.

### The TarP leucine-aspartic acid motif

Leucine-Aspartic acid motifs (LD-motifs) are well-recognised protein:protein interaction motifs [36], first identified in the FA protein paxillin, and shown to be required for paxillin to interact with focal adhesion kinase (FAK) [37]. The FAK–paxillin interaction was subsequently mapped to the focal adhesion targeting (FAT) domain of FAK [38]. It was reported previously that TarP contains an LD-motif (residues 655–680; TarP LD-motif) with sequence homology to paxillin LD2 [14], and that this LD-motif interacts with the FAK-FAT domain and plays a role in actin recruitment. The alignment of the TarP LD-motif with the LD domains in KANK1 [39], RIAM [40], DLC1 [20] and the paxillin LD1 and LD2 motifs are shown in Fig. 4A. To investigate the interaction of TarP LD-motif with FAK, we used the FP assay utilising fluorescein-labelled LD-motif peptides, and measured their binding to the FAK-FAT domain. As expected, paxillin LD2 bound well to the FAK-FAT domain

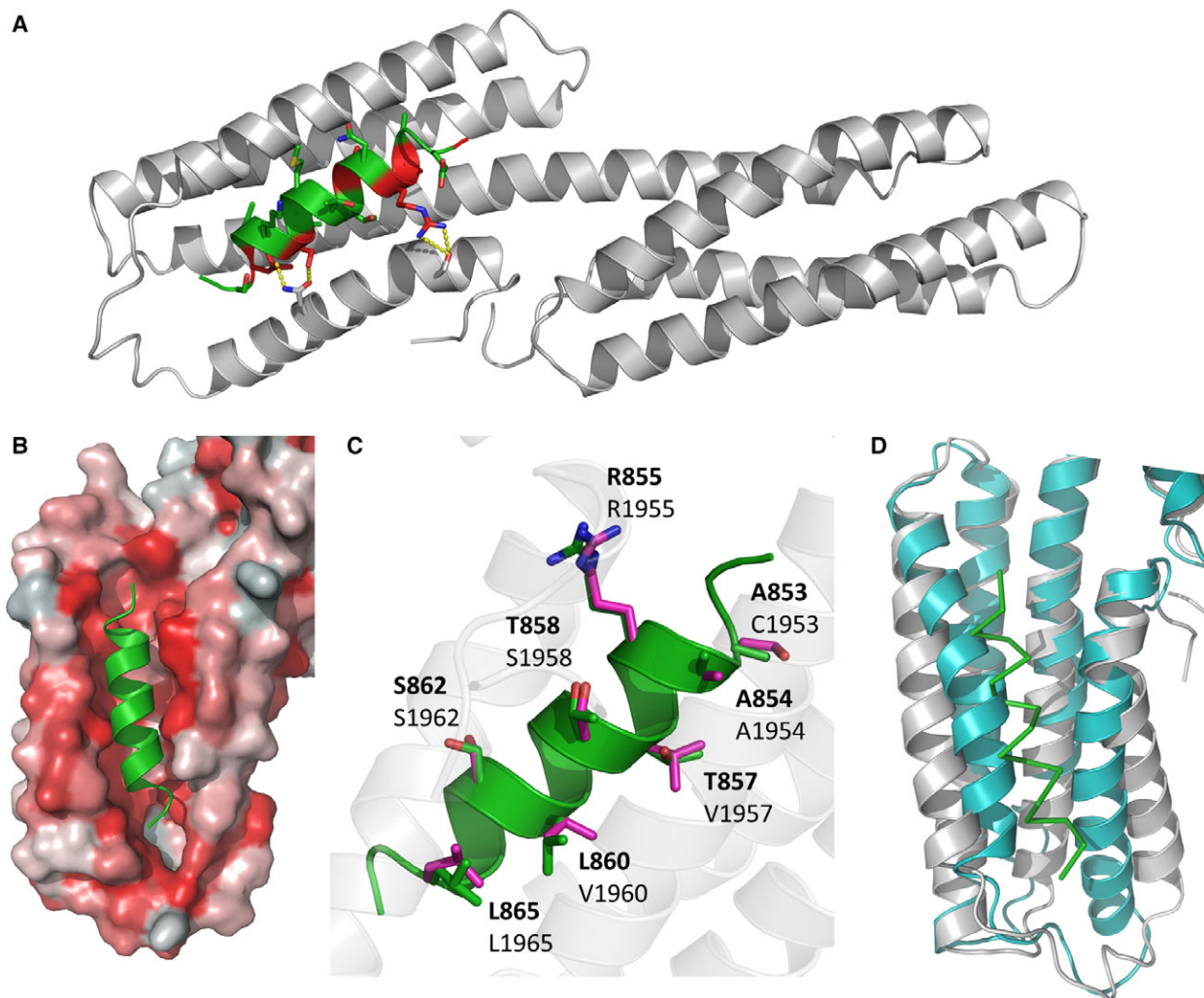


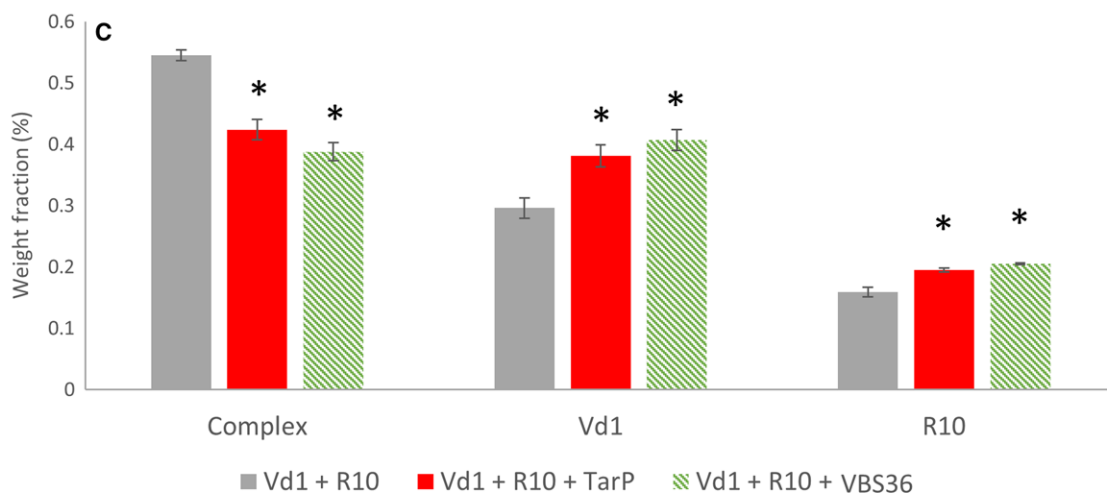
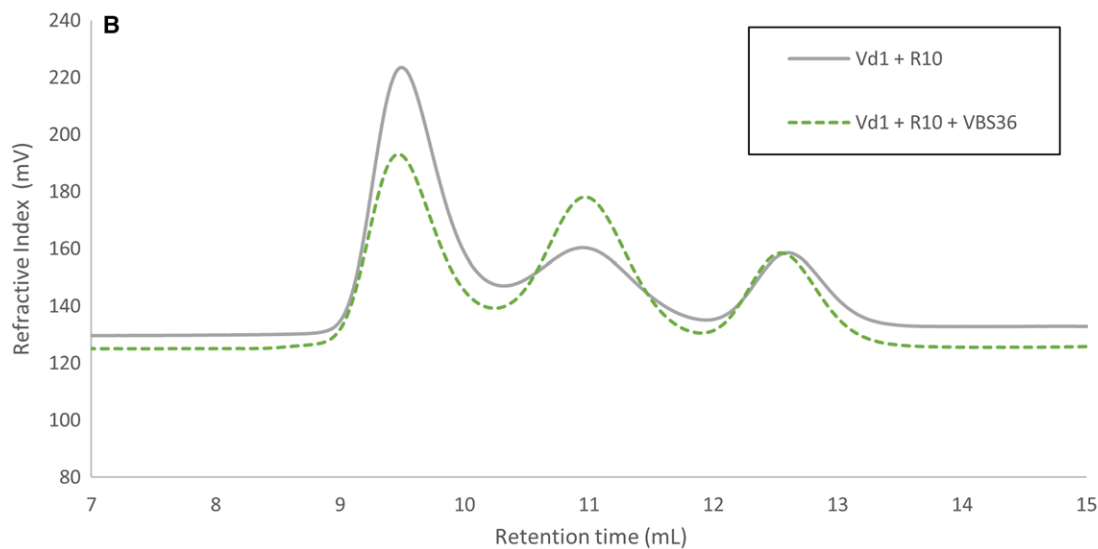
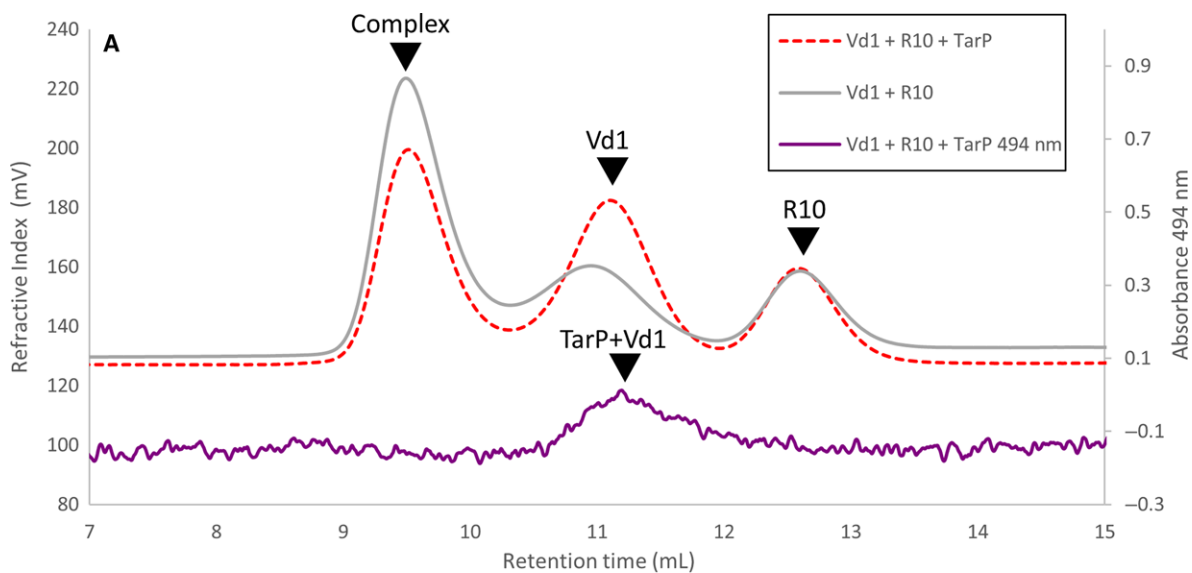
**Fig. 2.** Crystal structure of TarP in complex with Vd1. (A) Cartoon representation of the complex of Vd1 (grey) bound to TarP VBS (green); the consensus VBS residues are shown in red. (B) TarP VBS (green) docks into a hydrophobic groove on Vd1. Vd1 is represented as surface coloured by hydrophobicity: hydrophobic = red, hydrophilic = white. (C) TarP VBS peptide (green) aligned with talin VBS46 peptide (purple, PDB:1RKC [4]) with Vd1-interacting sidechains from both VBS shown as sticks and TarP residues (top bold) and corresponding vbs46 residues are shown. (D) VBS binding causes conformational change in the Vd1 domain. Comparison of apo Vd1 (cyan, PDB:1TR2 [45]) and TarP bound Vd1 (grey). The TarP peptide is shown as a ribbon (green).

( $K_d \sim 9 \mu\text{M}$ ) in line with previous reports [38]. However, we observed no increase in polarisation with the TarP LD-motif, suggesting that any interaction between TarP and FAK is too weak to be detected by the FP assay.

NMR is a powerful technique for studying interactions, even very weak (millimolar  $K_d$ ) interactions.

Addition of paxillin LD2 peptide to  $^{15}\text{N}$ -labelled FAK-FAT resulted in large chemical shift changes indicative of a robust interaction (Fig. 4C). In contrast, addition of a threefold excess of TarP LD-motif resulted in only very small shift changes, suggesting the peptide interacts only very weakly with FAK-FAT ( $K_d > \text{mM}$ ). This weak interaction explains the lack of

**Fig. 3.** TarP VBS disrupts the interaction between talin R10 and vinculin Vd1. Vd1 was incubated with talin R10 at 37 °C for 30 min then analysed on a gel filtration column (grey). The experiment was repeated with the addition of a stoichiometric amount of TarP VBS peptide (A) and then with talin VBS36 (B). All experiments were done in triplicate. 1% fluorescein-labelled TarP VBS peptide was added to monitor TarP VBS elution at 494 nm which confirmed that TarP eluted bound to Vd1 (purple). (C) the relative 'Weight Fraction' percentage for talin: vinculin complex, talin, vinculin peaks in the absence and presence of both TarP VBS and VBS36 peptides. Data are means  $\pm$  SEM; \* $P < 0.05$  by *T*-test. Both peptides reduced the R10-Vd1 complex.



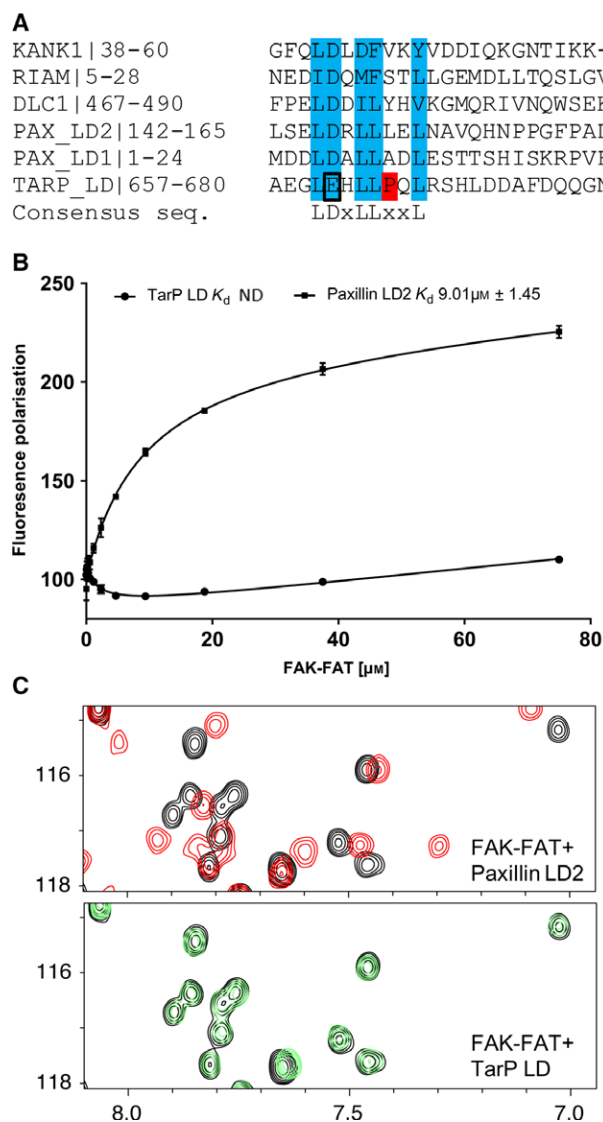


**Fig. 4.** The TarP LD-motif does not bind to FAK. (A) Multiple sequence alignment of known LD-motifs and TarP, generated using Clustal Omega; the consensus binding residues are highlighted in blue. (B) Binding of fluorescein-labelled TarP LD (655–680)C and Paxillin LD2 (141–153)C peptides to FAK-FAT, measured using a fluorescence polarisation assay. Dissociation constants  $\pm$  SE ( $\mu\text{M}$ ) for the interactions are indicated in the legend. ND, not determined. (C) 1H,15N-HSQC spectra of 130  $\mu\text{M}$  15N-labelled FAK-FAT in the absence (black) or presence of paxillin LD2 peptide (red; top panel) or TarP LD (green; bottom panel) at a ratio of 1 : 3.

binding in the FP experiment. The difference in binding affinity between the TarP LD-motif and paxillin LD2 to FAK-FAT may be explained by the presence of a proline residue, Pro675, in the middle of the TarP LD-motif (Fig. 4A). It is likely the proline destabilises and/or causes a kink in the  $\alpha$ -helix formed by the TarP LD-motif, but lack of binding might also be due to

the substitution of glutamate for aspartate in the ‘LD’ region of the TarP LD-motif. Therefore, despite the sequence homology, the TarP LD-motif binds much weaker than paxillin-LD2 to FAK-FAT, further refining the specificity determinants of LD-motifs and highlighting the fact that subtle changes in the sequence can significantly alter binding specificity.

It is possible that the TarP LD-motif may bind to another, currently unrecognised LD-binding domain protein, but it does not bind to FAK. Therefore, it seems likely that the TarP:FAK colocalisation reported previously *in cellulo* requires additional components that bring FAK and TarP together.

## Conclusions

In this study, we have further refined understanding of the molecular mechanisms underlying chlamydial infection *via* remodelling of the actin cytoskeleton; the ability of TarP to bind vinculin characterised here, and the recently characterised TarP WH2 motif that binds actin [41], look to be major components. Our data show that the constitutively active TarP VBS1 can out-compete the mechanosensitive interaction between talin and vinculin. Vinculin is a key player in the regulation of FA dynamics [42] and cell:cell junctions [43], and the capacity of TarP VBS1 to uncouple vinculin-mediated cytoskeletal connections during infection is therefore likely to have significant biological implications. Thus, it will be important to determine to what extent chlamydial infection alters the integrity and dynamics of cell:cell and cell:ECM junctions. Moreover, it raises the possibility that endogenous mammalian proteins might exist with constitutively active VBS, and that these could represent a new class of protein with the ability to regulate cell adhesion and migration.

## Acknowledgements

We thank Marie Anderson for help with the initial crystallography screen and David Critchley for critical reading of the manuscript. We also thank Diamond Light Source beamline I03 staff for their help in crystallographic data collection. B.T.G. is funded by BBSRC grant (BB/N007336/1) and HFSP grant (RGP00001/2016).

## Author contributions

BTG conceived and supervised the study; AJW and BTG designed experiments; AJW and AKS performed experiments; BTG, AJW, AKS and DGB analysed data; BTG and AJW wrote the manuscript.



## References

- Calderwood DA, Campbell ID and Critchley DR (2013) Talins and kindlins: partners in integrin-mediated adhesion. *Nat Rev Mol Cell Biol* **14**, 503–517.
- del Rio A, Perez-Jimenez R, Liu R, Roca-Cusachs P, Fernandez JM and Sheetz MP (2009) Stretching single talin rod molecules activates vinculin binding. *Science* (80-.) **323**, 638–641.
- Yao M, Goult BT, Klapholz B, Hu X, Toseland CP, Guo Y, Cong P, Sheetz MP and Yan J (2016) The mechanical response of talin. *Nat Commun* **7**, 11966.
- Izard T, Evans G, Borgon RA, Rush CL, Bricogne G and Bois PR (2004) Vinculin activation by talin through helical bundle conversion. *Nature* **427**, 171–175.
- Carisey A, Tsang R, Greiner AM, Nijenhuis N, Heath N, Nazgiewicz A, Kemkemer R, Derby B, Spatz J and Ballestrem C (2013) Vinculin regulates the recruitment and release of core focal adhesion proteins in a force-dependent manner. *Curr Biol* **23**, 271–281.
- le Duc Q, Shi Q, Blonk I, Sonnenberg A, Wang N, Leckband D and de Rooij J (2010) Vinculin potentiates E-cadherin mechanosensing and is recruited to actin-anchored sites within adherens junctions in a myosin II-dependent manner. *J Cell Biol* **189**, 1107–1115.
- Dos Reis RS and Horn F (2010) Enteropathogenic Escherichia coli, Salmonella, Shigella and Yersinia: cellular aspects of host-bacteria interactions in enteric diseases. *Gut Pathog* **2**, 8.
- Grove J and Marsh M (2011) The cell biology of receptor-mediated virus entry. *J Cell Biol* **195**, 1071–1082.
- Izard T, Tran Van Nhieu G and Bois PRJ (2006) Shigella applies molecular mimicry to subvert vinculin and invade host cells. *J Cell Biol* **175**, 465–475.
- Park H, Lee JH, Gouin E, Cossart P and Izard T (2011) The rickettsia surface cell antigen 4 applies mimicry to bind to and activate vinculin. *J Biol Chem* **286**, 35096–35103.
- Carabeo RA, Grieshaber SS, Fischer E and Hackstadt T (2002) Chlamydia trachomatis induces remodeling of the actin cytoskeleton during attachment and entry into HeLa cells. *Infect Immun* **70**, 3793–3803.
- Clifton DR, Fields KA, Grieshaber SS, Dooley CA, Fischer ER, Mead DJ, Carabeo RA and Hackstadt T (2004) From the cover: a chlamydial type III translocated protein is tyrosine-phosphorylated at the site of entry and associated with recruitment of actin. *Proc Natl Acad Sci* **101**, 10166–10171.
- Thwaites TR, Pedrosa AT, Peacock TP and Carabeo RA (2015) Vinculin interacts with the chlamydia effector TarP Via a tripartite vinculin binding domain to mediate actin recruitment and assembly at the plasma membrane. *Front Cell Infect Microbiol* **5**, 88.
- Thwaites T, Nogueira AT, Campeotto I, Silva AP, Grieshaber SS and Carabeo RA (2014) The Chlamydia effector TarP mimics the mammalian leucine-aspartic acid motif of paxillin to subvert the focal adhesion kinase during invasion. *J Biol Chem* **289**, 30426–30442.
- Banno A, Goult BT, Lee H, Bate N, Critchley DR and Ginsberg MH (2012) Subcellular localization of talin is regulated by inter-domain interactions. *J Biol Chem* **287**, 13799–13812.
- Vonrhein C, Flensburg C, Keller P, Sharff A, Smart O, Paciorek W, Womack T and Bricogne G (2011) Data processing and analysis with the *autoPROC* toolbox. *Acta Crystallogr D Biol Crystallogr* **67**, 293–302.
- Kabsch W (2010) XDS. *Acta Crystallogr D Biol Crystallogr* **66**, 125–132.
- Evans PR and Murshudov GN (2013) How good are my data and what is the resolution? *Acta Crystallogr D Biol Crystallogr* **69**, 1204–1214.
- Evans PR (2011) An introduction to data reduction: space-group determination, scaling and intensity statistics. *Acta Crystallogr D Biol Crystallogr* **67**, 282–292.
- Zacharchenko T, Qian X, Goult BT, Jethwa D, Almeida TB, Ballestrem C, Critchley DR, Lowy DR and Barsukov IL (2016) LD motif recognition by talin: structure of the Talin-DLC1 complex. *Structure* **24**, 1130–1141.
- McCoy AJ, Grosse-Kunstleve RW, Adams PD, Winn MD, Storoni LC and Read RJ (2007) *Phaser* crystallographic software. *J Appl Crystallogr* **40**, 658–674.
- Emsley P, Lohkamp B, Scott WG and Cowtan K (2010) Features and development of Coot. *Acta Crystallogr D Biol Crystallogr* **66**, 486–501.
- Murshudov GN, Skubák P, Lebedev AA, Pannu NS, Steiner RA, Nicholls RA, Winn MD, Long F and Vagin AA (2011) REFMAC5 for the refinement of macromolecular crystal structures. *Acta Crystallogr D Biol Crystallogr* **67**, 355–367.
- Chen VB, Arendall WB, Headd JJ, Keedy DA, Immormino RM, Kapral GJ, Murray LW, Richardson JS and Richardson DC (2010) MolProbity: all-atom structure validation for macromolecular crystallography. *Acta Crystallogr D Biol Crystallogr* **66**, 12–21.
- Krissinel E and Henrick K (2007) Inference of macromolecular assemblies from crystalline state. *J Mol Biol* **372**, 774–797.
- Gingras AR, Ziegler WH, Frank R, Barsukov IL, Roberts GCK, Critchley DR and Emsley J (2005) Mapping and consensus sequence identification for multiple vinculin binding sites within the talin rod. *J Biol Chem* **280**, 37217–37224.
- Hytönen VP and Vogel V (2008) How force might activate talin's vinculin binding sites: SMD reveals a structural mechanism. *PLoS Comput Biol* **4**, e24.

- 28 Yao M, Goult BT, Chen H, Cong P, Sheetz MP and Yan J (2015) Mechanical activation of vinculin binding to talin locks talin in an unfolded conformation. *Sci Rep* **4**, 4610.
- 29 Yan J, Yao M, Goult BT and Sheetz MP (2015) Talin dependent mechanosensitivity of cell focal adhesions. *Cell Mol Bioeng* **8**, 151–159.
- 30 Papagrigoriou E, Gingras AR, Barsukov IL, Bate N, Fillingham IJ, Patel B, Frank R, Ziegler WH, Roberts GC, Critchley DR *et al.* (2004) Activation of a vinculin-binding site in the talin rod involves rearrangement of a five-helix bundle. *EMBO J* **23**, 2942–2951.
- 31 Lee JH, Vornrhein C, Bricogne G and Izard T (2013) Crystal structure of the N-terminal domains of the surface cell antigen 4 of Rickettsia. *Protein Sci* **22**, 1425–1431.
- 32 Park H, Valencia-Gallardo C, Sharff A, Van Nhieu GT and Izard T (2011) Novel vinculin binding site of the IpaA invasin of shigella. *J Biol Chem* **286**, 23214–23221.
- 33 Bois PRJ, O'Hara BP, Nietlispach D, Kirkpatrick J and Izard T (2006) The vinculin binding sites of talin and  $\alpha$ -actinin are sufficient to activate vinculin. *J Biol Chem* **281**, 7228–7236.
- 34 Maartens AP, Wellmann J, Wictome E, Klapholz B, Green H and Brown NH (2016) *Drosophila* vinculin is more harmful when hyperactive than absent, and can circumvent integrin to form adhesion complexes. *J Cell Sci* **129**, 4354–4365.
- 35 Goult BT, Gingras AR, Bate N, Barsukov IL, Critchley DR and Roberts GCK (2010) The domain structure of talin: residues 1815–1973 form a five-helix bundle containing a cryptic vinculin-binding site. *FEBS Lett* **584**, 2237–2241.
- 36 Alam T, Alazmi M, Gao X and Arold ST (2014) How to find a leucine in a haystack? Structure, ligand recognition and regulation of leucine–aspartic acid (LD) motifs. *Biochem J* **460**, 317–329.
- 37 Thomas JW, Cooley MA, Broome JM, Salgia R, Griffin JD, Lombardo CR and Schaller MD (1999) The role of focal adhesion kinase binding in the regulation of tyrosine phosphorylation of paxillin. *J Biol Chem* **274**, 36684–36692.
- 38 Hoellerer MK, Noble MEM, Labesse G, Campbell ID, Werner JM and Arold ST (2003) Molecular recognition of paxillin LD motifs by the focal adhesion targeting domain. *Structure* **11**, 1207–1217.
- 39 Bouchet BP, Gough RE, Ammon Y-C, van de Willige D, Post H, Jacquemet G, Altelaar AM, Heck AJ, Goult BT and Akhmanova A (2016) Talin-KANK1 interaction controls the recruitment of cortical microtubule stabilizing complexes to focal adhesions. *Elife* **5**, e18124.
- 40 Goult BT, Zacharchenko T, Bate N, Tsang R, Hey F, Gingras AR, Elliott PR, Roberts GCK, Ballestrem C, Critchley DR *et al.* (2013) RIAM and vinculin binding to talin are mutually exclusive and regulate adhesion assembly and turnover. *J Biol Chem* **288**, 8238–8249.
- 41 Tolchard J, Walpole SJ, Miles AJ, Maytum R, Eaglen LA, Hackstadt T, Wallace BA and Blumenschein TMA (2018) The intrinsically disordered Tarp protein from chlamydia binds actin with a partially preformed helix. *Sci Rep* **8**, 1960.
- 42 Atherton P, Stutchbury B, Wang D-Y, Jethwa D, Tsang R, Meiler-Rodriguez E, Wang P, Bate N, Zent R, Barsukov IL *et al.* (2015) Vinculin controls talin engagement with the actomyosin machinery. *Nat Commun* **6**, 10038.
- 43 Yao M, Qiu W, Liu R, Efremov AK, Cong P, Seddiki R, Payre M, Lim CT, Ladoux B, Mège R-M *et al.* (2014) Force-dependent conformational switch of  $\alpha$ -catenin controls vinculin binding. *Nat Commun* **5**, 4525.
- 44 Jones DT and Cozzetto D (2015) DISOPRED3: precise disordered region predictions with annotated protein-binding activity. *Bioinformatics* **31**, 857–863.
- 45 Borgon RA, Vornrhein C, Bricogne G, Bois PR and Izard T (2004) Crystal structure of human vinculin. *Structure* **12**, 1189–1197.